Journal of University of Science and Technology Beijing
Volume 9, Number 4, August 2002, Page 311

Information

Analytical criteria for local activity of CNN with five state variables and application to Hyper-chaos synchronization Chua's circuit

Lequan Min and Xisong Dong

Applied Science School, University of Science and Technology Beijing, Beijing 100083, China
(Received 2002-04-10)

Abstract: The analytic criteria for the local activity theory in one-port cellular neural network (CNN) with five local state variables are presented. The application to a Hyper-chaos synchronization Chua's circuit (HCSCC) CNN with 1 125 variables is studied. The bifurcation diagrams of the HCSCC CNN show that they are slightly different from the smoothed CNN with one or two ports and four state variables calculated earlier. The evolution of the patterns of the state variables of the HCSCC CNN is stimulated. Oscillatory patterns, chaotic patterns, convergent or divergent patterns may emerge if the selected cell parameters are located in the locally active domains but nearby or in the edge of chaos domain.

Key words: cellular neural network; local activity; Hyper-Chaos Synchronization; Chua's circuit; five state variables; chaos

[*This project is jointly supported by the National Natural Science Foundation of China (Grant No. 60074034) and the Foundation for University Key Teacher by the Ministry of Education of China.*]

1 Introduction

The concept of local activity for reaction-diffusion CNN was first presented by Chua [1, 2]. The fundamental local activity theorem asserts that a wide spectrum of complex behaviors may exist if the corresponding cell parameters of a CNN are chosen in, or nearby, the edge of chaos domains. It has been successfully applied to various research areas in complex patterns and structures with significant physical, biological and engineering implications [3-16].

In this paper, the analytic criteria for testing the local activity of the CNN's with five state variables and one port are set up. As an application of the analytic criteria, a modified dual-layer two-dimensional reaction-diffusion CNN with one port and 1 125 arrays named HCSCC CNN has been introduced. The bifurcation diagrams of the HCSCC CNN have been calculated, which are slightly different from those of the modified dual-layer two-dimensional reaction-diffusion CNN with four state variables and one port or two ports [7, 12]. The numerical calculations show that the trajectories of the 1 125 local state variables of the HCSCC CNN can exhibit oscillatory patterns, chaotic patterns, or divergent patterns and with general synchronization characteristics if the selected cell parameters are located in the locally active unstable domains but nearby or in the edge of chaos domain.

Corresponding author: Lequan Min **E-mail:** lqmin@sohu.com

2 Analytical critria of local activity

For a one-port CNN cell, the corresponding local state equations with "5" state variables have the form:

$$\dot{\boldsymbol{V}}_a = \boldsymbol{A}_{aa}\boldsymbol{V}_a + \boldsymbol{A}_{ab}\boldsymbol{V}_b + \boldsymbol{I}_a, \tag{1}$$

$$\dot{\boldsymbol{V}}_b = \boldsymbol{A}_{ba}\boldsymbol{V}_a + \boldsymbol{A}_{bb}\boldsymbol{V}_b \tag{2}$$

where

$$\boldsymbol{V}_a = [V_1],\ \boldsymbol{V}_b = [V_2\ V_3\ V_4\ V_5]^T,\ \boldsymbol{I}_a = [I_1],$$

$$\boldsymbol{A}_{aa} = [a_{11}],\quad \boldsymbol{A}_{ab} = [a_{12}\,a_{13}\,a_{14}\,a_{15}],$$

$$\boldsymbol{A}_{ba} = \begin{bmatrix} a_{21} \\ a_{31} \\ a_{41} \\ a_{51} \end{bmatrix},\quad \boldsymbol{A}_{bb} = \begin{bmatrix} a_{22} & a_{23} & a_{24} & a_{25} \\ a_{32} & a_{33} & a_{34} & a_{35} \\ a_{42} & a_{43} & a_{44} & a_{45} \\ a_{52} & a_{53} & a_{54} & a_{55} \end{bmatrix}.$$

The corresponding CNN cell impedance $\boldsymbol{Z}_Q(s)$ is given by reference [1, 2]:

$$\begin{aligned} \boldsymbol{Z}_Q^{-1}(s) &= \boldsymbol{Y}_Q(s) \\ &= (s\boldsymbol{I}-\boldsymbol{A}_{aa}) - \boldsymbol{A}_{ab}(s\boldsymbol{I}-\boldsymbol{A}_{bb})^{-1}\boldsymbol{A}_{ba} \\ &= s - a_{11} - \frac{T_1 s^3 + K_1 s^2 + L_1 s + \Delta_1}{s^4 + Ts^3 + Ks^2 + Ls + \Delta} \end{aligned} \tag{3}$$

where $T, T_1, K, K_1, L, L_1, \Delta, \Delta_1$ are the functions of a_{ij}'s.

Lemma 1 [1, 2] A one-port reaction diffusion CNN cell is locally active at a cell equilibrium point Q if, and only if, its cell impedance at Q satisfies at least one of the following 4 conditions:

(1) $\boldsymbol{Y}_Q(s)$ has a pole in Re[s] > 0.

(2) $\boldsymbol{Y}^H_Q(\mathrm{i}\omega) = \boldsymbol{Y}^*_Q(\mathrm{i}\omega) + \boldsymbol{Y}_Q(\mathrm{i}\omega) < 0$ for some $\omega = \omega_0$, where ω_0 is any real number.

(3) $\boldsymbol{Y}_Q(s)$ has a simple pole $s = \mathrm{i}\omega_p$ on the imaginary axis, where its associated residue matirx

$$k_1 \triangleq \begin{cases} \lim\limits_{s\to \mathrm{i}\omega_p}(s-\mathrm{i}\omega_p)\boldsymbol{Y}_Q(s), & \text{if } \omega_p<\infty \\ \lim\limits_{\omega_p\to\infty}\boldsymbol{Y}_Q(\mathrm{i}\omega_p)/\mathrm{i}\omega_p, & \text{if } \omega_p=\infty \end{cases}$$

is either a complex number or a negative real number.

(4) $\boldsymbol{Y}_Q(s)$ has a multiple pole on the imaginary axis.

Definition 1 Define $a=[a_0,a_1,\cdots,a_{n-1}]$,

$p(s,a)=s^n+a_{n-1}s^{n-1}+\cdots+a_1s+a_0$,

$\mathcal{H}_n^+=\{a\in\mathbf{R}^n: p(s,a)=0\Rightarrow \mathrm{Re}[s]>0\}$.

Lemma 2 For any integer n,

(i) $\mathcal{H}_n\in\mathbf{R}^n$ is an open set.

(ii) $\mathcal{H}_n$ is a connected component of $\mathbf{R}^n\setminus\partial\mathcal{H}_n^+$.

Lemma 3 The boundary of $\mathcal{H}_n^+$, denoted by $\partial\mathcal{H}_n^+$, consists of $a\in\mathbf{R}^n$ such that $p(s,a)$ has at least one root in i$\mathbf{R}$.

Lemma 4

$\partial\mathcal{H}_4^+=\{[q_0q_2, q_1q_2, q_0+q_2, q_1]: q_0,q_1,q_2\geq 0\}$,

$\mathcal{H}_4^+=\{[a_0,a_1,a_2,a_3]: a_1a_2a_3>a_1^2+a_0a_3^2, a_0,a_1,a_2,a_3>0\}$.

Theorem 1 A necessary condition for

$$\boldsymbol{Y}_Q(s)=s-a_{11}-\frac{T_1s^3+K_1s^2+L_1s+\Delta_1}{s^4+Ts^3+Ks^2+Ls+\Delta}$$

to satisfy conditon 1 of Lemma 1 is

(I) $a\triangleq[\Delta,L,K,T]\in\mathbf{R}^4\setminus\{\mathcal{H}_4^+\cup\partial\mathcal{H}_4^+\}$.

A sufficient condition for $\boldsymbol{Y}_Q(s)$ to satisfy condition 1 in Lemma 1 is that $\boldsymbol{Y}_Q(s)$ satisfies condition (I) and one of the following conditions holds

(i) $T_1\neq 0$ and $[\Delta_1/T_1, L_1/T_1, K_1/T_1]\in\mathcal{H}_3^+\cup\partial\mathcal{H}_3^+$;

(ii) $T_1=0, K_1\neq 0$ and $[\Delta_1/K_1, L_1/K_1]\in\mathcal{H}_2^+\cup\partial\mathcal{H}_2^+$;

(iii) $T_1=0, K_1=0, L_1\neq 0$ and $[\Delta_1/L_1]\in\mathcal{H}_1\cup\partial\mathcal{H}_1$.

In order to set up the analytical criteria for Condition 2 in Lemma 1, the following equalilities are stated in advance:

$$h(\lambda)=-(TT_1-K_1)\lambda^3-Q\lambda^2-P\lambda-\Delta\Delta_1 \tag{4}$$

$$\lambda_j^*=\frac{Q+(-1)^j\sqrt{Q^2-3(TT_1-K_1)P}}{3(TT_1-K_1)},\ j=1,2 \tag{5}$$

$$Q=TL_1+LT_1-\Delta_1-KK_1 \tag{6}$$

$$P=LL_1-K\Delta_1-\Delta K_1 \tag{7}$$

$$E=-a_{11}, F=-TT_1+K_1-a_{11}(-2K+T^2) \tag{8}$$

$$G=-a_{11}(2\Delta+K^2-2LT)-\Delta_1+LT_1-KK_1+TL_1 \tag{9}$$

$$H=-a_{11}(-2\Delta K+L^2)-LL_1+K\Delta_1+K_1\Delta \tag{10}$$

$$I=-a_{11}\Delta^2-\Delta\Delta_1 \tag{11}$$

$$g(\Omega)=E\Omega^4+F\Omega^3+G\Omega^2+H\Omega+I \tag{12}$$

$$w_1=\frac{-1+\mathrm{i}\sqrt{3}}{2},\ w_2=\frac{-1-\mathrm{i}\sqrt{3}}{2} \tag{13}$$

$$\alpha_0=\frac{3F}{4E}, \beta_0=\frac{G}{2E} \tag{14}$$

$$p=-\frac{1}{3}\alpha_0^2+\beta_0 \tag{15}$$

$$q=\frac{2}{27}\alpha_0^3-\frac{\alpha_0\beta_0}{3}+\frac{H}{4E} \tag{16}$$

$$D=\frac{q^2}{4}+\frac{p^3}{27} \tag{17}$$

$$A_1=\{-q/2+D^{1/2}\}^{1/3} \tag{18}$$

$$A_2=\{-q/2-D^{1/2}\}^{1/3} \tag{19}$$

$$\Delta_1^*=A_1+A_2 \tag{20}$$

$$\Delta_2^*=w_1A_1+w_2A_2 \tag{21}$$

$$\Delta_3^*=w_2A_1+w_1A_2 \tag{22}$$

$$\Omega_1=\Delta_1^*-\alpha_0/3 \tag{23}$$

$$\Omega_2=\Delta_2^*-\alpha_0/3 \tag{24}$$

$$\Omega_3=\Delta_3^*-\alpha_0/3 \tag{25}$$

Theorem 2 Let the following parameters be defined *via* formulae (4)-(25), then $\boldsymbol{Y}^H_Q(\mathrm{i}\omega)<0$ for some $\omega=\omega_0\in\mathbf{R}$ if and only if at least one of the following condition holds.

(i) $a_{11}>0$.

(ii) $a_{11}=0$, $TT_1-K_1>0$.

(iii) $a_{11}=0, TT_1-K_1=0, \Delta_1-LT_1+KK_1-TL_1>0$.

(iv) $a_{11}=0, TT_1-K_1=0, \Delta_1-LT_1+KK_1-TL_1<0$, and $\Delta\Delta_1>0$.

(v) $a_{11}=0, TT_1-K_1=0, \Delta_1-LT_1+KK_1-TL_1<0, \Delta\Delta_1\leq 0$, $K\Delta_1+\Delta K_1-LL_1<0$, and

$$\Delta\Delta_1-\frac{(LL_1-K\Delta_1-\Delta K_1)^2}{4(\Delta_1-LT_1+KK_1-TL_1)}>0.$$

(vi) $a_{11}=0, TT_1-K_1=0, \Delta_1-LT_1+KK_1-TL_1=0$, and $LL_1-K\Delta_1-K_1\Delta>0$.

(vii) $a_{11}=0, TT_1-K_1=0, \Delta_1-LT_1+KK_1-TL_1=0$, $LL_1-K\Delta_1-K_1\Delta\leq 0$, and, $\Delta\Delta_1>0$.

(viii) $a_{11}=0, TT_1-K_1<0$, and, $\Delta\Delta_1>0$.

(ix) $a_{11}=0, TT_1-K_1<0$, and, $\Delta\Delta_1\leq 0$, but, $\lambda_1^*\geq 0$. and, $h(\lambda_1^*)<0$ or $\lambda_2^*\geq 0$ and $h(\lambda_2^*)<0$.

(x) $D>0, \Omega_1>0$ and $g(\Omega_1)<0$.

(xi) $D<0$, and

(a) $\Omega_1\geq 0$ and $g(\Omega_1)<0$ or

(b) $\Omega_2\geq 0$ and $g(\Omega_2)<0$ or

(c) $\Omega_3\geq 0$ and $g(\Omega_3)<0$.

(xii) $D=0, p=q=0, \alpha_0<0$, and $g(-\alpha_0/3)<0$.

(xiii) $D=0, q^2/4=-p^3/27\neq 0$, and

(a) $\Omega_1\geq 0, g(\Omega_1)<0$, or

(b) $\Omega_2\geq 0, g(\Omega_2)<0$.

Theorem 3 For $j=1, 2$, let

$w_j=(\sqrt{K+2\sqrt{\Delta}}+(-1)^j\sqrt{K-2\sqrt{\Delta}})/2$,

$w_j^*=\sqrt{(K+(-1)^j\sqrt{K^2-4\Delta})/2}$,

$A_j=L-3w_j^{*2}$,

$B_j=2Kw_j^*-4w_j^{*3}$,

$A_{1j}=\Delta_1-K_1w_j^{*2}$,

$B_{1j}=L_1w_j^*-T_1w_j^{*3}$,

$C=T(L_1-T_1K)-\Delta_1+KK_1$.

Then $\boldsymbol{Y}_Q(s)$ satisfies condition 3 in Lemma 1 if and only if one of the following conditions holds.

(i) If $\Delta>0, K>2\sqrt{\Delta}, T=L=0$, and

(a) $K_1w_1^2-\Delta_1\neq 0$, or

(b) $K_1w_1^2-\Delta_1=0$ and $\dfrac{L_1w_1-T_1w_1^3}{2w_1(w_2^2-w_1^2)}>0$, or

(c) $K_2w_2^2-\Delta_1\neq 0$, or

(d) $K_2w_2^2-\Delta_1=0$ and $\dfrac{L_1w_2-T_1w_2^3}{2w_2(w_1^2-w_2^2)}>0$.

(ii) $K>0, \Delta_1T\neq 0, \Delta=0, L=KT$ and $\Delta_1/KT<0$.

(iii) $\sqrt{K}c\neq 0$.

(iv) $C=0$ and $\dfrac{T(\Delta_1-KK_1)+K(L_1-T_1K)}{2K(T^2+K)}<0$.

(v) $\Delta=0$ and $\Delta_1L>0$,

(vi) $\Delta\neq 0, K^2-4\Delta>0, L=T(K+\sqrt{K^2-4\Delta})/2$, or $L=T(K-\sqrt{k^2-4\Delta})/2$, and

(a) $A_jB_{1j}-A_{1j}B_j\neq 0$, or

(b) $A_jB_{1j}-A_{1j}B_j=0$ and $\dfrac{A_jA_{1j}-B_{1j}B_j}{A_j^2+B_j^2}>0$.

Theorem 4 $\boldsymbol{Y}_Q(s)$ has a multiple pole on the imaginary axis if and only if the following conditions hold.

(i) $L=\Delta=0, \Delta_1\neq 0$.

(ii) $L=\Delta=K=0, \Delta_1\neq 0$.

(iii) $L=\Delta=K=T=0, K_1\neq 0, \Delta_1\neq 0$.

(iv) $T=L=0, K>0, \Delta=(K/2)^2$.

3 HCSCC CNN and its bifurcation diagrams

Firstly, a HCSCC CNN with one port and 15×15 arrays is introduced which is similar to the one given in [11]. It has been found that these HCSCC CNN's might be the most friendly models, which either have very complex dynamical behaviors or are studied easily *via* the local activity principle.

The HCSCC equations are represented as follows.

$$\frac{dx_1}{dt}=\alpha[x_2-x_1-bx_1-\frac{(a-b)}{\pi}\arctan(5x_1)] \tag{26}$$

$$\frac{dx_2}{dt}=x_1-x_2+x_3 \tag{27}$$

$$\frac{dx_3}{dt}=-\beta x_2 \tag{28}$$

$$\frac{dx_4}{dt}=\cos^2(x_4)[x_1+x_3-\tan(x_4)] \tag{29}$$

$$\frac{dx_5}{dt}=\cos^2(x_5)[-\beta x_2.+x_3-\tan(x_5)] \tag{30}$$

where α, β, a and b are parameters.

Now let us map the HCSCC Equations (26)-(30) into a 2-dimensional 15×15 HCSCC CNN with one port (one diffusion constant D_1):

$$\dot{x}_{1i,j}=\alpha[x_{2i,j}-x_{1i,j}-bx_{1i,j}-\frac{(a-b)}{\pi}\arctan(5x_{1i,j})]+ D_1[x_{1i+1,j}+x_{1i-1,j}+x_{1i,j+1}+x_{1i,j-1}-4x_{1i,j}] \tag{31}$$

$$\dot{x}_{2i,j}=x_{1i,j}-x_{2i,j}+x_{3i,j} \tag{32}$$

$$\dot{x}_{3i,j}=-\beta x_{2i,j} \tag{33}$$

$$\dot{x}_{4i,j}=\cos^2(x_{4ij})[x_{1ij}+x_{3ij}-\tan(x_{4ij})] \tag{34}$$

$$\dot{x}_{5i,j}=\cos^2(x_{5ij})[x_{2ij}+x_{3ij}-\tan(x_{5ij})],\quad i,j=1, 2,\cdots, 15, \tag{35}$$

In component form, equations (31)-(35) become

$$\dot{\boldsymbol{X}}_1=f_1(\boldsymbol{X}_1,\boldsymbol{X}_2,\boldsymbol{X}_3,\boldsymbol{X}_4,\boldsymbol{X}_5)+D_1\nabla^2\boldsymbol{X}_1 \tag{36}$$

$$\dot{\boldsymbol{X}}_2=f_2(\boldsymbol{X}_1,\boldsymbol{X}_2,\boldsymbol{X}_3,\boldsymbol{X}_4,\boldsymbol{X}_5) \tag{37}$$

$$\dot{\boldsymbol{X}}_3=f_3(\boldsymbol{X}_1,\boldsymbol{X}_2,\boldsymbol{X}_3,\boldsymbol{X}_4,\boldsymbol{X}_5) \tag{38}$$

$$\dot{\boldsymbol{X}}_4=f_4(\boldsymbol{X}_1,\boldsymbol{X}_2,\boldsymbol{X}_3,\boldsymbol{X}_4,\boldsymbol{X}_5) \tag{39}$$

$$\dot{\boldsymbol{X}}_5=f_5(\boldsymbol{X}_1,\boldsymbol{X}_2,\boldsymbol{X}_3,\boldsymbol{X}_4,\boldsymbol{X}_5) \tag{40}$$

where

$f_1(\boldsymbol{X}_1,\boldsymbol{X}_2,\boldsymbol{X}_3,\boldsymbol{X}_4,\boldsymbol{X}_5)=$
$\alpha[\boldsymbol{X}_2-\boldsymbol{X}_1-b\boldsymbol{X}_1-\dfrac{(a-b)}{\pi}\arctan(5\boldsymbol{X}_1)]$.

$f_2(\boldsymbol{X}_1,\boldsymbol{X}_2,\boldsymbol{X}_3,\boldsymbol{X}_4,\boldsymbol{X}_5)=\boldsymbol{X}_1-\boldsymbol{X}_2+\boldsymbol{X}_3$.

$f_3(\boldsymbol{X}_1,\boldsymbol{X}_2,\boldsymbol{X}_3,\boldsymbol{X}_4,\boldsymbol{X}_5)=-\beta\boldsymbol{X}_2$.

$f_4(\boldsymbol{X}_1,\boldsymbol{X}_2,\boldsymbol{X}_3,\boldsymbol{X}_4,\boldsymbol{X}_5)=\cos^2(\boldsymbol{X}_4)[\boldsymbol{X}_1+\boldsymbol{X}_3-\tan(\boldsymbol{X}_4)]$.

$f_5(\boldsymbol{X}_1,\boldsymbol{X}_2,\boldsymbol{X}_3,\boldsymbol{X}_4,\boldsymbol{X}_5)=\cos^2(\boldsymbol{X}_5)[-\beta\boldsymbol{X}_2+\boldsymbol{X}_3-\tan(\boldsymbol{X}_5)]$.

and ∇^2 corresponds to a 225×225 matrix.

The cell equilibrium points Q_i's of equations (36)-(40) for the restricted local activity domain [3] can be determined *via* equations:

$$f_1(X_1, X_2, X_3, X_4, X_5) = 0 \quad (41)$$

$$f_2(X_1, X_2, X_3, X_4, X_5) = 0 \quad (42)$$

$$f_3(X_1, X_2, X_3, X_4, X_5) = 0 \quad (43)$$

$$f_4(X_1, X_2, X_3, X_4, X_5) = 0 \quad (44)$$

$$f_5(X_1, X_2, X_3, X_4, X_5) = 0 \quad (45)$$

From equations (41)-(45), it can be concluded that for any parameter group $\{\alpha, \beta, a, b\}$, there exists at least one cell equilibrium point Q_1= (0, 0, 0, 0, 0). On the other hand, any other cell equilibrium point Q_i = $(x_1, x_2, x_3, x_4, x_5)$ must satisfy the following equations.

$$x_2 = 0, \ x_3 = -x_1 \quad (46)$$

$$(1+b)x_1 + \frac{(a-b)}{\pi}\arctan(5x_1) = 0 \quad (47)$$

$$\cos^2(x_4)\tan(x_4) = 0 \quad (48)$$

$$\cos^2(x_5)[x_1 + \tan(x_5)] = 0 \quad (49)$$

Consequently, it can be obtained by the following constraint condition.

Constraint condition: If Q_2 is a nonzero equilibrium point, then $Q_3 = -Q_2$ is also an equilibrium point, and the parameters a and b have to satisfy the inequality

$$(b+1) < 5(b-a)/\pi \quad (50)$$

From equations (46)-(49), it follows that the other nonzero cell equilibrian points have the form:

$$Q_2 = [x_1, 0, -x_1, k\pi, -\arctan x_1],$$

$$Q_3 = [x_1, 0, -x_1, \pi/2 + k\pi, -\arctan x_1],$$

$$Q_4 = [x_1, 0, -x_1, k\pi, \pi/2 + k\pi],$$

$$Q_5 = [x_1, 0, -x_1, \pi/2 + k\pi, \pi/2 + k\pi],$$

where x_1 is determined by equation (47), and $k = 0, \pm 1, \pm 2, \cdots$.

The cell coefficients $a_{m,n}(Q_i)$'s are defined *via* the corresponding Jacobian matrix and is given as follows:

$$A_i \triangleq \begin{bmatrix} a_{11}(Q_i) & a_{12}(Q_i) & a_{13}(Q_i) & a_{14}(Q_i) & a_{15}(Q_i) \\ a_{21}(Q_i) & a_{22}(Q_i) & a_{23}(Q_i) & a_{24}(Q_i) & a_{25}(Q_i) \\ a_{31}(Q_i) & a_{32}(Q_i) & a_{33}(Q_i) & a_{34}(Q_i) & a_{35}(Q_i) \\ a_{41}(Q_i) & a_{42}(Q_i) & a_{43}(Q_i) & a_{44}(Q_i) & a_{45}(Q_i) \\ a_{51}(Q_i) & a_{52}(Q_i) & a_{53}(Q_i) & a_{54}(Q_i) & a_{55}(Q_i) \end{bmatrix}$$

$$= \begin{bmatrix} a_{11}(Q_i) & a_{12}(Q_i) & 0 & 0 & 0 \\ a_{21}(Q_i) & a_{22}(Q_i) & a_{23}(Q_i) & 0 & 0 \\ 0 & a_{32}(Q_i) & 0 & 0 & 0 \\ a_{41}(Q_i) & 0 & a_{43}(Q_i) & a_{44}(Q_i) & 0 \\ 0 & a_{52}(Q_i) & a_{53}(Q_i) & 0 & a_{55}(Q_i) \end{bmatrix} \quad (51)$$

where

$$a_{11} = \alpha\{-1 - [b + \frac{5(a-b)}{\pi(1+(5x_1)^2)}]\}, \ a_{12} = \alpha, \quad (52)$$

$$a_{21} = 1, \ a_{22} = -1, \ a_{23} = 1, \ a_{32} = -\beta, \ a_{41} = \cos^2 x_4, \quad (53)$$

$$a_{43} = \cos^2 x_4, \ a_{44} = -\cos(2x_4) - (x_1 + x_3)\sin(2x_4) \quad (54)$$

$$a_{52} = -\beta\cos^2 x_5, \ a_{53} = \cos^2 x_5,$$

$$a_{55} = -\cos(2x_5) - (-\beta x_2 + x_3)\sin(2x_5) \quad (55)$$

Using Theorems 1-4, constrain condition (50), and formulae (3)-(4), (51)-(55) the locally active domains, and edges of chaos of the HCSCC with respect to the equilibrium points Q_1 with different cell parameters is the same as those shown in figure 1 (a) in [11]. The bifurcation diagrams of the HCSCC with respect to equilibrium ponits Q_2 and Q_i (i=3, 4, 5) are shown in **figures 1(a) and 1(b)**, respectively.

From these graphs, it can be concluded that:

- For all the selected parameter groups, the corresponding bifurcation diagrams do not have locally

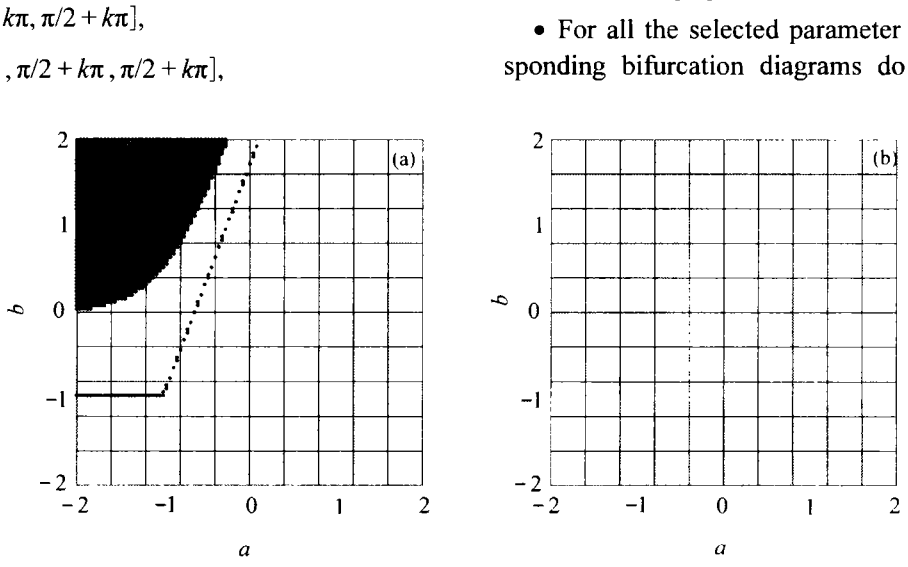

Figure 1 Bifurcation diagrams of the HCSCC CNN with parameters α = 10 and β = 15. Edge of chaos domain (black), locally active and unstable domain (gray). In the domaim coded with white, no nonzero equilibrium point exists. Equilibrium points (a) Q_2 and (b) Q_i (i=3, 4, 5).

passive domains.

• The bifurcation graphs of the HCSCC with respect to Q_i ($i = 3, 4, 5$) are the same as that shown in figure 1 (b).

4 Dynamic simulations of HCSCC CNN's

Now let us deal with the 15×15 HCSCC CNN's with the periodic boundary condition and choose, in equations (31)-(35), a parameter group $\{\alpha, \beta\} = \{10, 15\}$. Firstly, let us simulate the dynamic patterns of the HCSCC equations. Our simulation results are listed in **table 1**. The numerical simulation have shown that the qualitative behaviors of the HCSCC Equations (26)-(30) and the HCSCC CNN's are similar if the diffusion parameters D_1 is small enough. Roughly speaking, if the parameters a and b are selected in the edge of chaos (black) of the equilibrium Q_2 shown in figure 1(a), the dynamic behaviors of the corresponding HCSCC CNN's might be oscillatory, chaotic, or convergent (see table 1), depending on initial conditions. If the parameters a and b are chosen in the inner region of the locally active domain (gray) shown in figure 1 (a), the corresponding SCC CNN's may exhibit successively chaotic or oscillatory patterns, chaotic or divergent patterns, and convergent or divergent patterns, depending on initial conditions. In the domain which does not satisfy the constrain condition (50), oscillatory, divergent or convergent patterns may be generated, depending on initial condintions and the locations of the patameters a and b (see table 1).

Table 1 Cell parameters, equilibrium points Q_i's and the dynamic properties of HCSCC CNN's

No.	a	b	Equilibrium point	Pattern
1*	−1.2	1.00	0.3806, 0, −0.3806, 0, 0.3637	⇓○
2*	−1.2	0.31	0.4097, 0, −0.4097, 0, 0.3889	⇓○
3*	−1.2	0.30	0.4104, 0, −0.4104, 0, 0.3894	⇓⊕○
4	−1.2	0.29	0.4110, 0, −0.4110, 0, 0.3900	⇑⊕○
5	−1.2	−0.08	0.4450, 0, −0.4450, 0, 0.4187	⊕○
6	−1.2	−0.91	1.4727, 0, −1.4727, 0, 0.9743	⇑⊕
7	−1.2	−0.94	2.0313, 0, −2.0313, 0, 1.1133	⇓⇑
8	−1.2	−0.99	10.3711, 0, −10.3711, 0, 1.4747	⇓
9	−1.4	−1.50	0, 0, 0, 0, 0	⇑
10*	−1.4	2.00	0.3991, 0, −0.3991, 0, 0.3797	⇓
11*	−1.4	0.19	0.5920, 0, −0.5920, 0, 0.5345	⇓⊕○
12	−1.4	0.17	0.5118, 0, −0.5118, 0, 0.4731	⊕○
13	−1.4	0.10	0.5234, 0, −0.5234, 0, 0.4822	⊕○
14	−1.4	−0.92	2.8670, 0, −2.8670, 0, 1.2352	⇑⊕
15	−1.4	−0.93	3.2248, 0, −3.2248, 0, 1.2701	⇑○
16	−1.4	−0.94	3.7016, 0, −3.7016, 0, 1.3069	⇑⇓
17	−1.4	−0.96	5.3696, 0, −5.3696, 0, 1.3867	⇓
18	1.0	−1.00	0, 0, 0, 0, 0	⇓○

Note: Fixed parameters $\{\alpha, \beta\} = \{10, 15\}$, $D_1 = 0.01$. The symbols ⇑, ⇑, ○, and ⊕ indicate convergent, divergent, periodic and chaotic patterns, respectively. i* represents that the cell parameters lie on the edge of chaos domain.

Figures 2 and 3 exhibit, respectively, chaotic and oscillatory trajectories generated *via* the HCSCC equations numbered by 3 listed in table 1 with different initial conditions $(x_1(0), x_2(0), x_3(0), x_4(0), x_5(0)) = (0.1, 0.1, 0.1, 0.1, 0.1)$ and $(x_1(0), x_2(0), x_3(0), x_4(0), x_5(0)) = (-0.8828, -0.1004, 6.1887, -\arctan(0.1004), \text{atan}(6.19887))$. **Figures 4 and 5** exhibit, respectively, chaotic and divergent trajectories generated *via* the HCSCC equations numbered by 6 listed in table 1 with different initial conditions $(x_1(0), x_2(0), x_3(0), x_4(0), x_5(0)) = (0.1, 0.1, 0.1, 0.1, 0.1)$ and $(x_1(0), x_2(0), x_3(0), x_4(0), x_5(0)) = (10, 10, 10, 10, 10)$.

Now, let us simulate their corresponding 15×15 SCC CNN's with periodic boundary conditions.

• The patterns generated by the parameter group No. 3. The parameter group is located in the the edge of chaos with respect to the equilibrium point Q_2 (see figure 1 (a)). **Figure 6** shows the chaotic trajectories of the components of states $X_{17,7}$, $X_{27,7}$, $X_{37,7}$, $X_{47,7}$, $X_{57,7}$,of the HCSCC CNN are very similar to those of the original HCSCC equations (see figure 2). If the gray-scale color code for the components of the solution of the HCSCC CNN is defined by **figure 7**. The graphs of the time evolution of the patterns of the local state variables of the HCSCC CNN over the time interval [0, 120] is shown in **figure 8**. The diffusion parameter D_1

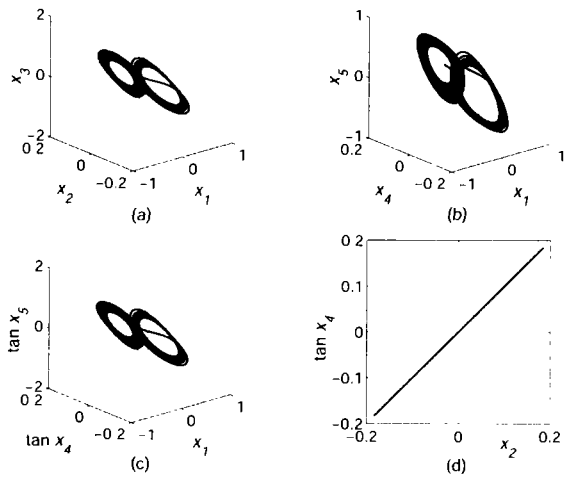

Figure 2 The generalized chaotic synchronization, (a) The trajectory of variables x_1, x_2 and x_3; (b) The trajectory of variables x_1, x_4 and x_5; (c) The decoded trajectory of variables x_1, x_4 and x_5 which is the same as that shown in (a); (d) Variables x_1 and x_4 are in generalized chaotic synchronization *via* the transformation $\tan(x_4)$.

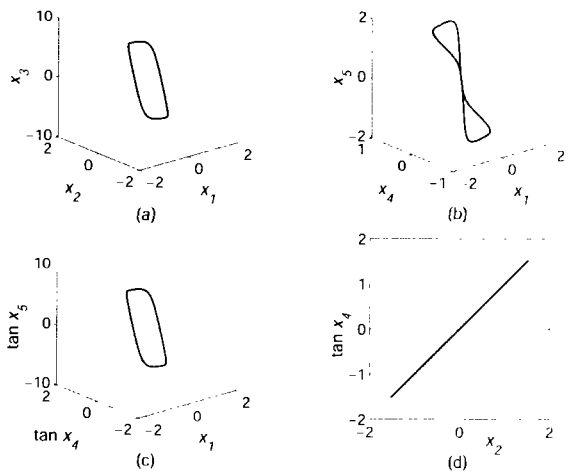

Figure 3 The generalized periodic synchronization, (a) The trajectory of variables x_1, x_2 and x_3; (b) The trajectory of variables x_1, x_4 and x_5; (c) The decoded trajectory of variables x_1, x_4 and x_5 which is the same as that shown in (a); (d) Variables x_1 and x_4 are in generalized chaotic synchronization *via* the transformation $\tan(x_4)$.

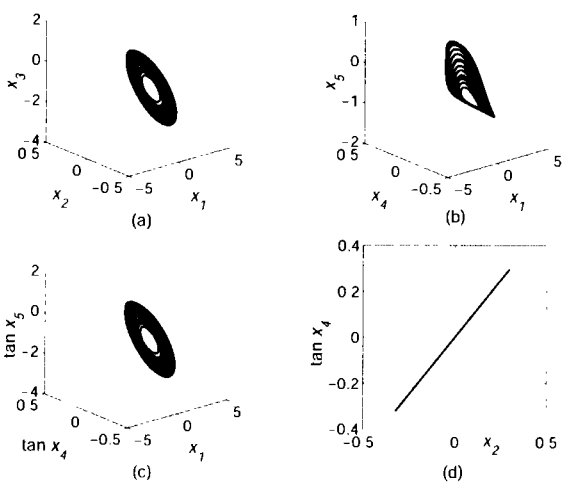

Figure 4 The generalized chaotic synchronization; (a) The trajectory of variables x_1, x_2 and x_3; (b) The trajectory of variables x_1, x_4 and x_5; (c) The decoded trajectory of variables x_1, x_4 and x_5 which is the same as that shown in (a); (d) Variables x_1 and x_4 are in generalized chaotic synchronization *via* the transformation $\tan(x_4)$.

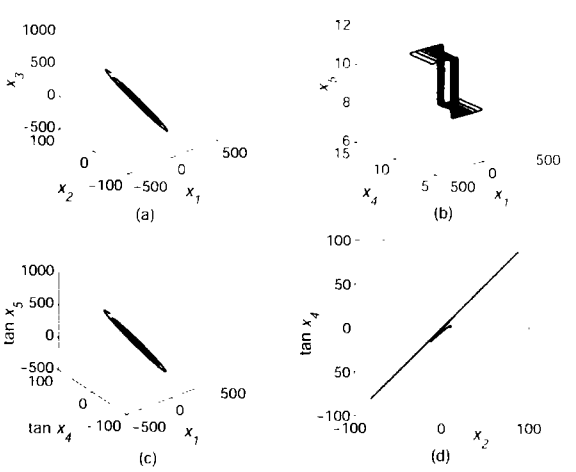

Figure 5 The generalized divergent synchronization, (a) The trajectory of variables x_1, x_2 and x_3; (b) The trajectory of variables x_1, x_4 and x_5; (c) The decoded trajectory of variables x_1, x_4 and x_5 which is the same as that shown in (a); (d) Variables x_1 and x_4 are in generalized divergent synchronization *via* the transformation $\tan(x_4)$.

is selected as 0.01. The initial condition is chosen as follows.

$$x_{1i,j}(0) = \begin{cases} 0.1, & \text{if } i+j=\text{even} \\ -0.1, & \text{otherwise.} \end{cases}$$

$$x_{2i,j}(0) = \begin{cases} 0.1, & \text{if } i+j=\text{even} \\ -0.1, & \text{otherwise.} \end{cases}$$

$$x_{3i,j}(0) = \begin{cases} 0.1, & \text{if } i+j=\text{even} \\ -0.1, & \text{otherwise.} \end{cases}$$

$$x_{4i,j}(0) = \begin{cases} \arctan(0.1), & \text{if } i+j=\text{even} \\ -\arctan(0.1), & \text{otherwise.} \end{cases}$$

$$x_{5i,j}(0) = \begin{cases} \arctan(0.1), & \text{if } i+j=\text{even} \\ -\arctan(0.1), & \text{otherwise.} \end{cases}$$

In summary, the HCSCC CNN's introduced in this paper are, in fact, hyper-chaotic synchronization systems and have extremly complex dynamic behaviors. In particular, the emergence of complex patterns of the HCSCC CNN's can be observed if the corresponding cell parameters chosen nearby the boundary of the edge of chaos or the unstable active domain.

5 Concluding remarks

The research on emergence and complex has gained

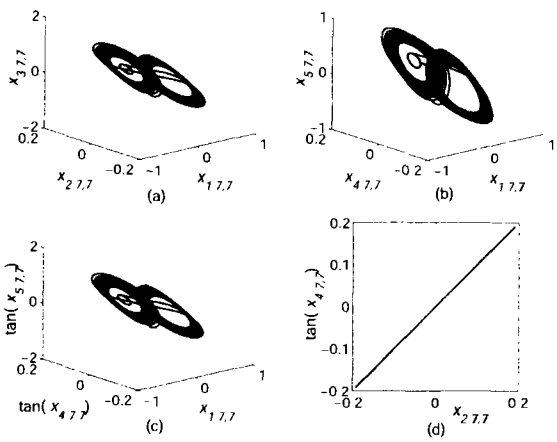

Figure 6 The generalized hyper-chaotic synchronization. The trajectory of the components of the state variables X_1, X_2, X_3, X_4, X_5: (a) $x_{17,7}, x_{27,7}$ and $x_{37,7}$; (b) The trajectory of variables $x_{17,7}, x_{47,7}$ and $x_{57,7}$; (c) The decoded trajectory of variables $x_{17,7}, x_{47,7}$ and $x_{57,7}$ which is the same as that shown in (a); (d) Variables $x_{17,7}$ and $x_{47,7}$ are in generalized chaotic synchronization *via* the transformation $\tan(x_{47,7})$.

Figure 7 The gray-scale color code for the components of the solution of the HCSCC CNN state equations, $G_{i,j}$ stands for $x_{1i,j}, x_{2i,j}, x_{3i,j}, x_{4i,j}$ or $x_{5i,j}$.

much attention during the past decade. Chaos, as a special complex dynamical phenomenon, has been studied for more than four decades. However, determination, prediction, and control of copmlex patterns generated from higher-dimensional nonlinear systems are still very difficult issues. The local activity principle of the CNN has provided a powerful tool for studying the emergence of complex patterns of a kind of nonlinear systems.

Based on Lemma 1 of the local activity principle of CNN cells presented by Chua [1, 2], the analytical criteria of the local activity for CNN's with five state variables and one-port (one diffusion coefficient) are set up. The analytical criteria consist of Theorems 1-4, which can be implemented by a computer program to produce bifurcation diagrams for general corresponding CNNs.

An HCSCC CNN with 1 125 variables is intoduced. The theory for constructing generalized synchronization of vector equations [17] motivates us to develope such an HCSCC CNN system although a strict new theory should be proposed to verify mathematically that the HCSCC CNN does have generalized synchronization. According to the bifurcation diagrams, generalized synchronic chaotic patterns, oscillatory patterns of the HCSCC CNN's can be easily simulated numerically. Our results imply that the local activity theory of CNN is also a practical tool for the study of the complex dynamics of some hyper-chaos generalized synchronization nonlinear systems.

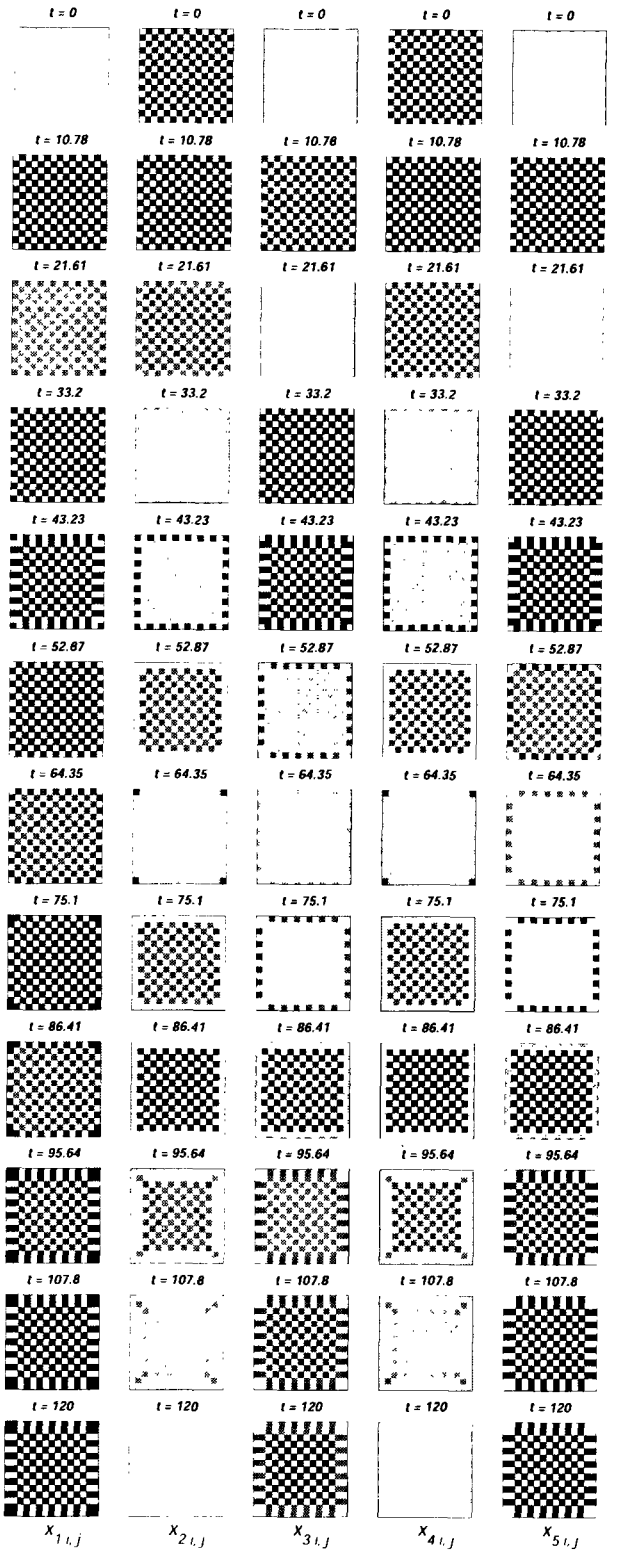

Figure 8 Evolution of the patterns of the state variables of No. 3 HCSCC CNN listed in table 1.

Clearly, further researches on the hyper-chaos gener-

alized synchronization are very promising both in practical and theoretical views of points.

References

[1] L.O. Chua, CNN: a vision of complexity [J], *Int. J. Bifurcation and Chaos*, 7 (1997), No.10, p.2219.

[2] L.O. Chua, Passivity and complexity [J], *IEEE Trans. Circuits Syst. I: Fundamental Theory and Applications*, 46 (1999), p. 71.

[3] R. Dogaru and L.O. Chua, Edge of chaos and local activity domain of FitzHugh-Nagumo equation [J], *Int. J. Bifurcation and Chaos*, 8 (1998), No.2, p.211.

[4] R. Dogaru and L.O. Chua, Edge of chaos and local activity domain of the Brussselator CNN [J], *Int. J. Bifurcation and Chaos*, 8 (1998), No.6, p.1107.

[5] R. Dogaru and L.O. Chua, Edge of chaos and local activity domain of Gierer-Meinhardt CNN [J], *Int. J. Bifurcation and Chaos*, 8 (1998), No.12, p.2321.

[6] L. Min, K.R. Crounse, and L. O. Chua, Analytical criteria for local activity and applications to the Oregonator CNN [J], *Int. J. Bifurcation and Chaos*, (2000), No.1, p.25.

[7] L. Min, K.R. Crounse, and L.O. Chua, Analytical criteria for local activity of reaction-diffusion CNN with four state variables and applications to the Hodgkin-Huxley equation [J], *Int. J. Bifurcation and Chaos*, 10 (2000), No.6, p.1295.

[8] L. Min, Theorem for testing local activity of CNN and application to cardiac Purkinje equations [J], *J. Univ. Sci. Technol. Beijing*, 7 (2000), No.2, p.139.

[9] L. Min and N. Yu, Analytical criteria for local Activity of CNN with two-port and application to biochemical model [J], *J. Univ. Sci. Technol. Beijing*, 7 (2000), No.4, p.305.

[10] L. Min and N. Yu, Theorems for testing local activity of CNN with two-ports and applications to smoothed Chua's circuit [J], *Advances in Systems Science and Applications*, (2000), No.2, p.51.

[11] L. Min and J. Wang, Local activity of coupled Duffing equation and numerical simulation [J], *J. Univ. Sci. Technol. Beijing* (in Chinese), 23 (2001), Special Issue, p.9.

[12] N. Yu and L. Min, Analytical criteria for local activity of CNN with two ports and application to Smoothed Chua's Circuits [J], *J. Univ. Sci. Technol. Beijing*, 9 (2002), No.1, p.65.

[13] L. Min and J. Wang, Theory for local activity of three-port CNN with four state variables [J], *J. Univ. Sci Technol. Beijing* (in Chinese), 24 (2002), No.1 p.79.

[14] L. Min, X. Dong, and N. Yu, Applications for local activity of three-port CNN with four state variables to the equations of growth of tumor [J], *J. Univ. Sci. Technol. Beijing* (in Chinese), 24 (2002), No.3, p.372.

[15] L. Min and N. Yu, Some analytical criteria for local activity of two-port CNN with threeor four state variables: analysis and applications [J], *Int. J. Bifurcation and Chaos*, 12 (2002), No.5, p.931.

[16] L. Min and N. Yu, Application of local activity theory of the cellular neural network with two ports to the coupled Lorenz-cell Model [J], *Communications in Theoretical Physics*, 37 (2002), No.6, p.759.

[17] X. Zhang and L. Min, Theory for constructing generalized synchronization and applications [J], *J. Univ. Sci. Technol. Beijing*, 7 (2000), No.3, p.225.